



LUND UNIVERSITY

High-gain Soft-x-ray Pumped Photoionization Laser in Zinc Vapor

Lundberg, Hans; Macklin, J. J; Silfvast, W. T; Wood, O. R

Published in:
Applied Physics Letters

DOI:
[10.1063/1.95260](https://doi.org/10.1063/1.95260)

1984

[Link to publication](#)

Citation for published version (APA):

Lundberg, H., Macklin, J. J., Silfvast, W. T., & Wood, O. R. (1984). High-gain Soft-x-ray Pumped Photoionization Laser in Zinc Vapor. *Applied Physics Letters*, 45(4). <https://doi.org/10.1063/1.95260>

Total number of authors:
4

General rights

Unless other specific re-use rights are stated the following general rights apply:

Copyright and moral rights for the publications made accessible in the public portal are retained by the authors and/or other copyright owners and it is a condition of accessing publications that users recognise and abide by the legal requirements associated with these rights.

- Users may download and print one copy of any publication from the public portal for the purpose of private study or research.
- You may not further distribute the material or use it for any profit-making activity or commercial gain
- You may freely distribute the URL identifying the publication in the public portal

Read more about Creative commons licenses: <https://creativecommons.org/licenses/>

Take down policy

If you believe that this document breaches copyright please contact us providing details, and we will remove access to the work immediately and investigate your claim.

LUND UNIVERSITY

PO Box 117
221 00 Lund
+46 46-222 00 00

High-gain soft-x-ray-pumped photoionization laser in zinc vapor

H. Lundberg, J. J. Macklin, W. T. Silfvast, and O. R. Wood, II
AT&T Bell Laboratories, Holmdel, New Jersey 07733

(Received 7 May 1984; accepted for publication 5 June 1984)

Large inversion densities in Zn^+ have been produced by photoionizing inner-shell d electrons with the broadband soft-x-ray flux from a $1.06\text{-}\mu\text{m}$ laser-produced plasma. This pumping scheme is an effective technique for rapidly producing large population densities ($5 \times 10^{13} \text{ cm}^{-3}$) in the $3d^9 4s^2 {}^2D_{5/2}$ upper laser level. These large densities (a) produced laser action on a two-electron transition from the d -electron manifold to the outer-electron manifold at 7478 \AA , (b) allowed the isotope shifts on this relatively weak transition to be measured, and (c) may eventually be transferred to other high lying states in Zn^+ to produce vacuum ultraviolet lasers.

A high-intensity soft-x-ray flux from a laser-produced plasma source has been used to photoionize and consequently produce large population inversions in Zn vapor. The broadband soft-x-ray emission removes a d electron from the Zn atom leaving it in an inner-shell ionic state which is inverted with respect to a lower lying Zn^+ state. This selective pumping scheme produced laser action on a two-electron transition from the d -electron manifold to the outer electron manifold at 7478 \AA and allowed the isotope shifts on this relatively weak transition to be measured for the first time. Inversion densities as high as $5 \times 10^{13} \text{ cm}^{-3}$ have been measured, making these inner-shell Zn^+ levels an attractive source of excited ions from which to transfer energy and, thereby, make short wavelength lasers.

Soft-x-ray-pumped photoionization lasers were recently reported¹ in Cd vapor at 4416 and 3250 \AA . Gains as high as 5.6 cm^{-1} and inversion densities greater than $1 \times 10^{14} \text{ cm}^{-3}$ were obtained in Cd by the inner-shell photoionization process. Laser action took place in Cd vapor adjacent to a high-temperature blackbody source of soft x rays produced by focusing the output from a $1.06\text{-}\mu\text{m}$ laser onto a solid target² located in a Cd heat pipe. The success of this pumping scheme in Cd depended on the high photoionization cross section³ (15 Mb) for removal of the inner d -electron. The same pumping scheme can be applied in Zn, since Cd and Zn have an identical electronic configuration in their outer shell.

An energy-level diagram for a photoionization laser in Zn is shown in Fig. 1. The outer electronic configuration of the Zn atom ground state is $3d^{10} 4s^2 {}^1S_0$ and the state pumped by photoionization is the identical electronic arrangement with one d -electron removed, $3d^9 4s^2 {}^2D_{5/2,3/2}$. A calculated cross section⁴ for producing this state (the sum of the $5/2$ and $3/2$ contributions) by photoionization is shown in Fig. 2 as the solid curve between 30 and 725 \AA . The peak value for this cross section (10 Mb) occurs at a wavelength of 190 \AA . Other calculations⁵ and a comparison between theoretical and experimental values for Cd and Hg indicate, however, that the d -electron cross section could be at least a factor of 2 lower. The lower peak cross section for Zn (as compared to Cd) and the shift to shorter wavelength are expected to make this laser system approximately 2.5 times less efficient than Cd for the same $1.06 \mu\text{m}$ input laser intensity.

The experimental arrangement for producing the Zn^+

laser was almost identical to that used previously in Cd.¹ A 2.5-cm -diam heat pipe in the form of a cross was used to provide Zn vapor at pressures from 1 to 10 Torr ($500\text{--}600^\circ\text{C}$). The Zn pressure was determined by a curve-of-growth technique⁶ in which the length of the hot zone was taken to be 10 cm . A 300-mJ , 10-ns pulse from a Nd:yttrium aluminum garnet laser, focused with a 25-cm focal length lens through one arm of the cross onto a rotating tungsten target inside the heat pipe, created a plasma which provided the source of soft x rays. The $1.06\text{-}\mu\text{m}$ laser intensity, approximately 10^{11} W/cm^2 , is expected to produce a soft-x-ray flux with an approximate 13-eV blackbody distribution lasting for the duration of the laser pulse.¹ The excellent match between the distribution of the source (dashed curve) and the spectral dependence of the photoionization cross section for d -electron removal is shown in Fig. 2. An expanding plasma of the target material was observed to enter the laser gain region some $20\text{--}30 \text{ ns}$ after the laser pulse was over (depending upon the distance from the target material). Laser action was observed along the other axis of the cross where Brewster-angle windows were fitted to the ends of the heat pipe. Gain at 7478 \AA along this axis of the cross was determined by (a) measuring the ratio of the emission at that wavelength with and without a rear mirror present⁷, (b) observing large enhancements when an optical resonator was installed

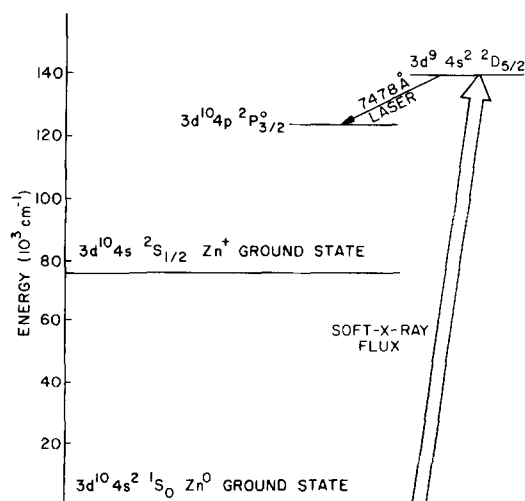


FIG. 1. Energy-level diagram showing inner-shell photoionization of Zn vapor.

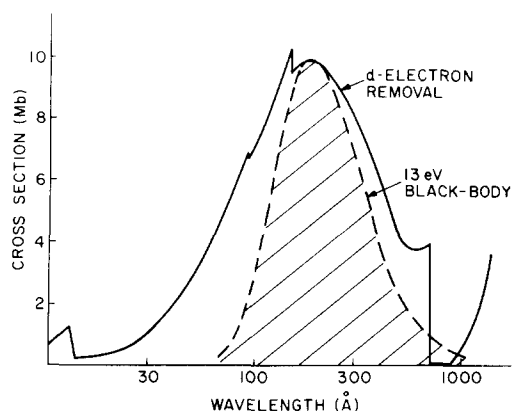


FIG. 2. Calculated photoionization cross section vs wavelength for Zn vapor (solid curve) where the region between 30 and 725 Å depicts *d*-electron removal, and calculated emission spectrum of a 13-eV blackbody (dashed curve).

around the plasma, and (c) probing the gain region directly with a dye laser.

Measurements of the gain-length product (GL) in Zn^+ at 7478 Å were made at various Zn pressures, 1.06-μm laser energies, and distances above the target surface. This was done using method (a) above, where the ratio of double-pass to single-pass emission provides a direct measure of the GL product. The highest value of GL observed corresponds to a gain coefficient of 2.2 cm^{-1} over an estimated length of 1 cm. This gain was observed 5 mm from the target at the largest 1.06-μm input energy (300 mJ) and the highest Zn pressure (10 Torr). For a fixed height (5 mm) and pressure (10 Torr), the GL product was found to increase linearly with 1.06-μm laser intensity. For a fixed height (5 mm) and input energy (300 mJ) GL rises linearly with Zn pressure up to 10 Torr and then remains approximately constant. For a fixed pressure and energy (10 Torr, 300 mJ), the GL product displays a dependence on height similar to that found earlier in Cd^+ , i.e., rises sharply to its peak value at 5 mm from the target then falls off more slowly with increasing distance from the target. When an optical resonator was installed along the axis of the heat pipe, measurements with and without the rear resonator mirror gave intensity ratios as high as 10^5 . This ratio leads to a gain estimate that is consistent with the single-mirror results when the number of passes during the average gain pulse duration (between 10–20 ns) is taken into account. In addition, a pulse from a dye laser tuned to 7478 Å was found to be amplified by a factor of 5 when passed through the Cd vapor near the soft-x-ray source. This result is also consistent with the emission ratio measurements provided the wider linewidth of the dye laser is taken into account.

The linewidth and isotope shifts on the laser transition must be considered when determining the maximum population from the measured gain. Because of the two-electron nature of the laser transition ($3d^9 4s^2 {}^2D_{5/2} - 3d^{10} 4p {}^2P_{3/2}$) large isotope shifts are possible. The isotope shift at 7478 Å was not known but the isotope shift on the related weaker transition (${}^2D_{3/2} - {}^2P_{1/2}$) at 5894 Å had been previously measured⁸ (laser action was not observed on this transition). Although the isotope shifts on these two transitions are expect-

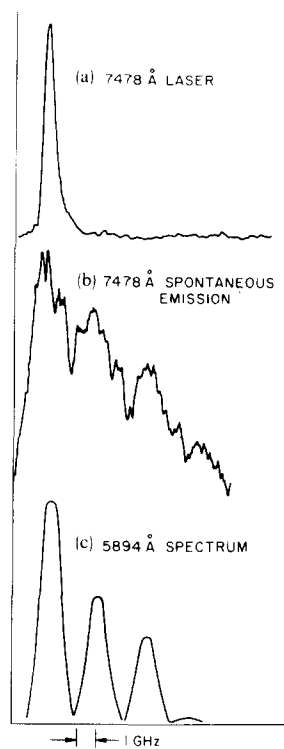


FIG. 3. Experimental measurement of stimulated emission on the 7478 Å transition (a) with resonator and (b) without resonator showing isotopic distribution. For comparison, previously measured isotopic distribution on (c) the 5894-Å transition in the same multiplet.

ed to be reasonably similar, a line shape measurement was made at 7478 Å to enable the determination of the absolute density of the ${}^2D_{5/2}$ state produced by the soft-x-ray source, to check the consistency of the isotope shifts at various wavelengths and to determine if other broadening effects were playing a role in this photoionized plasma. Measurements of the frequency distribution of the emission at 7478 Å obtained using a scanning Fabry-Perot interferometer are shown in Fig. 3. The spectrum of the laser emission at 7478 Å, obtained when an optical resonator surrounded the heat pipe, is shown in Fig. 3(a). For this measurement the interferometer, which was fitted with highly reflecting mirrors, had an instrument resolution of approximately 0.5 GHz. The frequency spectrum of the spontaneous emission at 7478 Å is shown in Fig. 3(b). For this measurement the interferometer, which was fitted with partially transmitting mirrors in order to preserve an acceptable signal-to-noise ratio, had an instrument resolution approaching 1 GHz. A frequency spectrum for the 5894-Å transition, calculated using a linewidth based on Doppler broadening and isotope shifts taken from the results of a previous measurement⁸, is shown in Fig. 3(c).

The isotope shifts at 7478 Å [Fig. 3(b)] are in almost exact agreement with those at 5894 Å [Fig. 3(c)], as are the relative intensities determined by the isotopic abundance of the three strongest isotopes of Zn (48% – $Z = 64$, 28% – $Z = 66$, and 18% – $Z = 68$). The measurement of laser emission at 7478 Å [Fig. 3(a)] indicates a complete dominance by the strongest ($Z = 64$) isotope. This is expected since the gain for that isotope is almost a factor of 2 greater than for the next most abundant isotope. The bandwidth of the stimulated emission is narrower than the bandwidth of the spontaneous emission because the higher gain at the center of the Doppler profile strongly enhances the emission at those frequencies with multiple passes through the

gain medium. Since the observed broadening is not significantly different from that expected for Doppler broadening even though the plasma electron density is high (10^{14} cm^{-3}), it appears that line broadening is not a significant factor in this pumping scheme.

Since the isotope shifts are greater than the Doppler width of the transition, each isotope will behave as a separate laser species. Because of this the population in the upper laser level, determined from the gain measurement, must be multiplied by the reciprocal of the largest isotope fraction to determine the total population of all isotopes. Therefore, the measured gain coefficient (2.2 cm^{-1}) leads to a value for the population density in the upper laser state of $5 \times 10^{13} \text{ cm}^{-3}$. Knowledge of the population density in these states will be useful in future energy-transfer experiments in which population in the 2D state is transferred to the outer electron manifold via narrow frequency lasers tuned to these and sim-

ilar isotopically shifted core-linking transitions. For example, transferring the population in the 2D states to higher states in Zn^+ with a tunable UV laser could produce inversions from those states with respect to the $4p$ level. Such a scheme could result in lasers at wavelengths as short as 1200 \AA .

¹W. T. Silfvast, J. J. Macklin, and O. R. Wood, II, *Opt. Lett.* **8**, 551(1983).

²R. G. Caro, J. C. Wang, R. W. Falcone, J. R. Young, and S. E. Harris, *Appl. Phys. Lett.* **42**, 9(1983).

³R. B. Cairns, H. Harrison, and R. I. Schoen, *J. Chem. Phys.* **51**, 5440(1969).

⁴E. J. McGuire, Technical Memorandum SC-TM-68-70, Sandia Laboratories, Albuquerque, New Mexico, January, 1968.

⁵W. R. Johnson, V. Radojević, P. Deshmukh, and K. T. Cheng, *Phys. Rev. A* **25**, 337(1982).

⁶A. Corney, *Atomic and Laser Spectroscopy* (Clarendon, Oxford, 1977), p.300.

⁷W. T. Silfvast and J. S. Deech, *Appl. Phys. Lett.* **11**, 97 (1967).

⁸R. Kloch, Z. Les, D. N. Stacey, V. Stacey, *Acta Phys. Pos. A* **61**, 483(1982).

Effect of active layer placement on the threshold current of $1.3\text{-}\mu\text{m}$ InGaAsP etched mesa buried heterostructure lasers

N. K. Dutta, R. J. Nelson,^{b)} R. B. Wilson,^{b)} D. M. Maher, P. D. Wright,^{b)} T. T. Sheng, P. S. D. Lin,^{a)} and R. B. Marcus^{a)}

AT&T Bell Laboratories, Murray Hill, New Jersey 07974

(Received 20 April 1984; accepted for publication 4 June 1984)

The threshold current of InGaAsP etched mesa buried heterostructure (EMBH) lasers is strongly influenced by the position of the active layer in the etched mesa. Transmission electron microscopy results are presented which show the presence of a thin planar disorder along the etched 111A interface. Nonradiative recombination of carriers is believed to be responsible for the increased threshold current of EMBH lasers whose active region is bounded by 111A interface. Lasers with threshold current as low as 14 mA at 30°C have been fabricated by proper placement of the active layer and by optimizing layer thicknesses and doping levels.

Real index guided lasers are needed as sources for high bit rate fiber communication systems. Several different types of real index guided laser structures using the InGaAsP/InP material system have been fabricated at various research laboratories over the last few years.¹⁻⁶ Most of this work has concentrated on lasers emitting at 1.3 and $1.55 \mu\text{m}$ because the silica optical fibers exhibit zero dispersion at $1.3 \mu\text{m}$ and have lowest loss at $1.55 \mu\text{m}$. The lasers emitting at $1.3 \mu\text{m}$ are characterized by low threshold ($20\text{--}30 \text{ mA}$), high efficiency ($\sim 0.2\text{--}0.25 \text{ mW/mA/facet}$), and good light-current linearity. Optimization of layer thicknesses, dopings, and layer placement are necessary in order to fabricate these low threshold high performance lasers.⁷ This paper reports the effect on the threshold current of the placement of the active layer relative to the other layers in etched mesa buried heterostructure (EMBH) lasers.^{2,3} Transmission electron microscopy (TEM) results are presented which show that high-

er thresholds in some EMBH lasers are associated with a defect structure at the edge of an active region which is in contact with a 111A interface. Lasers with low threshold current have been fabricated by optimum placement of the active layer.

The schematic cross section of an EMBH laser is shown in Fig. 1(a). The device fabrication involves the following steps.^{2,3} A planar InGaAsP-InP double heterostructure layer is grown by liquid phase epitaxy (LPE) on a n -InP substrate, followed by $\text{Br}_2\text{--CH}_3\text{OH}$ etching of a dovetail-shaped mesa and then LPE regrowth. The side walls of the etched mesa are approximately the crystallographic 111A (In rich) planes. Figures 1(b), 1(c), and 1(d) illustrate three different cases of the position of the active layer relative to the neck of the mesa.

We find that lasers with active layer placed above the neck of the mesa have higher threshold current [Fig. 1(d)] than lasers with active layer below the neck [Fig. 1(c)]. Figure 2 shows the threshold current of individual lasers plotted

^{a)} Bell Communication Research.

^{b)} Work done while at Bell Laboratories.